NOVEL TIME INTEGRATORS APPLIED TO NON-LINEAR REAL TIME AND PSEUDO-DYNAMIC TESTS

O.S. Bursi[1], L. He[2], L. Vulcan[2], P. Pegon[3] and D.J. Wagg[4]

[1] *Professor, Dept. of Mechanical and Structural Engineering, University of Trento, Trento, Italy*
[2] *Research Assistant, Dept. of Mechanical and Structural Engineering, University of Trento, Trento, Italy*
[3] *Researcher, European Laboratory for Structural Assessment, EC JRC, Ispra, Italy*
[4] *Reader in Dynamics and Control, Department of Mechanical Engineering, University of Bristol, Bristol, UK*
E-mail: oreste.bursi@ing.unitn.it, leqia.he@ing.unitn.it, leonardo.vulcan@ing.unitn.it, pierre.pegon@jrc.it, david.wagg@bristol.ac.uk

ABSTRACT:

Real-time testing with dynamic substructuring (RTDS) is a novel form of hybrid numerical-experimental testing technique used to simulate structures subjected to seismic loadings. By imposing compatibility and equilibrium conditions at the interface between the numerical substructure and the physical substructure, respectively, the substructures are made to interact in real time. In this paper, first we show the application to non-linear hybrid tests of L-stable Real Time compatible integrators derived from Rosenbrock methods. These algorithms are competitive in terms of stability and accuracy when applied to real time and stiff problems. In detail, the non-linear specimen considered is a spring pendulum coupled to a linear or a non-linear numerical oscillator implemented by means of the Bouc-Wen model. We also present a novel interfield parallel partitioned method applied to pseudo-dynamic (PsD) tests with dynamic substructuring (DS). In detail, the proposed coupling algorithm enables arbitrary Generalized-α schemes to be coupled with different time steps in each subdomain and represents an extension of an interfield parallel method originally proposed by Pegon and Magonette. Numerical experiments highlight the improved performance of the novel method in PsD simulations with respect to its progenitor.

KEYWORDS: Real time dynamic substructuring, real time compatible integrator, partitioned integrator, generalized-α methods

1. INTRODUCTION

RTDS is a novel form of heterogeneous numerical-experimental technique which can be used to test structural systems under dynamic loading (Williams *et al.* 2001). The technique involves splitting the system being tested into two parts: the physical substructure (PS) and the numerical substructure (NS). The physical specimen is typically built only for the part where damage is expected whilst the remainder is numerically simulated. By imposing compatibility and equilibrium conditions at the interface, the substructures are made to interact in real time in order to emulate the dynamic behaviour of the whole system. To interconnect the PS to the NS, a transfer system that acts on the PS is typically controlled to follow the NS interface kinematic quantities or other outputs (Wallace *et al.* 2005). At the same time, the force between the transfer system and the PS is fed back as an input to the NS. This entire process must take place in real time. This leads to a key challenge: to run the test in real time a real-time compatible (RTC) integrator is required, i.e. a scheme which does not require the knowledge of the state and of the coupling force ahead of the current stage of the time step (Bursi *et al.* 2008). In this paper, we extend linearly implicit noniterative fixed stepsize integrators (Burgermeister et al., 2006) to Rosenbrock-based schemes applied to non-linear systems. Therefore, a prediction-substitution procedure based on kinematic control and without iteration to satisfy the real time requirement (Bursi *et al.* 2008) is considered hereinafter. The interaction between subsystems is schematically depicted in Figure 1. The numerical procedure entails the integration of the differential equations of the NS using the coupling force u^n_{k-1} available at t_{k-1}; the motion of the actuator governed by predicted kinematic quantity u^p_k available at t_k and the subsequent measuring of the coupling force $z^p_{k+1} = u^p_{k+1}$.

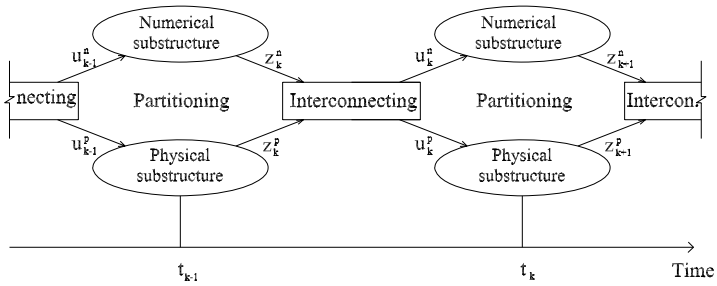

Figure 1 Interaction in real time and force-kinematic (mixed) coupling strategy after Bursi et al. (2008)

Within the context of coupled dynamic systems, partitioned time integration schemes that are explicit-implicit and/or multi-time-step for different substructures are very appealing for the continuous PsD testing with DS. Gravouil and Combescure (2001) conceived a multi-time-step coupling method, labelled the GC method herein, able to couple arbitrary Newmark-β schemes with different time steps in different subdomains. The staggered procedure of the GC is a serious drawback in PsD tests, as the PS integrated with fine time steps has to systematically stop to wait for the NS treated with coarse time steps. To solve this issue, Pegon and Magonette (2002) developed and implemented an interfield parallel algorithm, the PM method, based on the GC method, but where the NS and the PS states advance simultaneously and continuously. The interfield parallel solution procedure of the PM method is schematically illustrated in Figure 2. In detail, subdomain A is discretized in time with a coarse time step Δt_A; subdomain B is integrated with a fine time step Δt_B associated with $\Delta t_A = ss\Delta t_B$, being ss the number of substeps. In order to send in advance information to subdomain B at the end of a coarse time step, the PM method exploits a time step equal to $2\Delta t_A$.

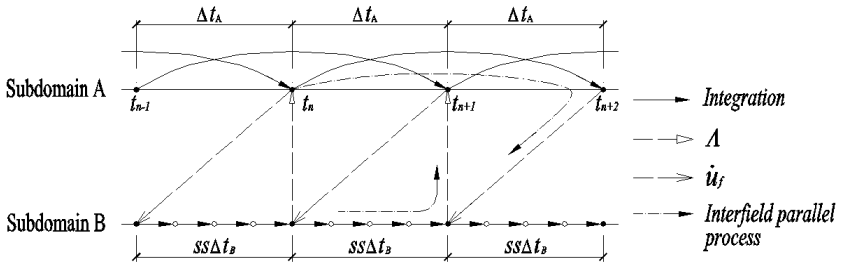

Figure 2 The interfield parallel solution procedure after Pegon and Magonette (2002)

This paper presents shortly the novel L-stable algorithms for real time testing and the PM method for PsD testing with relevant applications. In detail, in Section 2 we introduce L-stable algorithms and their applications to non-linear RTDS testing. Conversely in Section 3, we present a novel interfield parallel method that relies on the powerful Generalized-α methods (Chung and Hulbert, 1993), in short the G-α methods, and relevant numerical experiments that illustrate the performance of the novel method. Conclusions are drawn in Section 4.

2. L-STABLE INTEGRATORS FOR REAL-TIME TESTING

In this section, we briefly introduce novel real time compatible algorithms for RTDS tests. The convergence analysis of these algorithms applied to linear cases can be found in Bursi *et al.* (2008). The extension to the non-linear case is illustrated hereinafter.

2.1. L-stable real-time compatible integrators

Real time compatibility of an integrator implies that a numerical method does not require the knowledge of *f* or its derivatives at the end of the time step Δt for the solution of the differential equation *y'=f(y,t)* (Bursi *et al.* 2008). Moreover, to be compatible with let's say a real time dSPACE controller board, the integrator has to be characterized by intermediate sub-steps sampled with a sample rate equal to an integer number of the base

sample rate (dSPACE 2001). Therefore, the conceived linearly implicit algorithm uses only values or measurements at the beginning or inside Δt. Herein, two- and three-stage L-stable real-time compatible and noniterative algorithms derived from Rosenbrock (1963) with fixed time steps, that are second- and third-order accurate, respectively, for monolithic and linear problems, are introduced. By using an s-stage Rosenbrock method one obtains,

$$\begin{aligned} \mathbf{y}_{k+1} &= \mathbf{y}_k + \sum_{i=1}^{s} b_i \mathbf{k}_i \\ \mathbf{k}_i &= \left[\mathbf{I} - \gamma \Delta t \mathbf{J}\right]^{-1} \left[\mathbf{f}\left(t_k + \alpha_i \Delta t, \mathbf{y}_k + \sum_{j=1}^{i-1} \alpha_{ij} \mathbf{k}_j \right) + \mathbf{J} \sum_{j=1}^{i-1} \gamma_{ij} \mathbf{k}_j \right] \Delta t \end{aligned} \tag{2.1}$$

where $\alpha_i = \sum_{j=1}^{i-1} \alpha_{ij}$, γ_{ij} and b_i are the algorithm coefficients and **J** is the Jacobian operator at the beginning of Δt. A linear equation system has to be solved at every stage and the Jacobian needs to be updated at the beginning of each Δt only in the non-linear case. For the two-stage L-stable (LSRT2) method we propose the parameters reported here,

$$\gamma = -\gamma_{21} = 1 - \sqrt{2}/2, \ \alpha_2 = \alpha_{21} = 1/2, \ b_1 = 0, \ b_2 = 1 \tag{2.2}$$

Relevant parameters for the three-stage L-stable (LSRT3) method can be found in Bursi *et al.* (2008).
In order to appraise the accuracy of these algorithms, the algorithmic damping ratio $\bar{\xi}$ and the algorithmic damped numerical frequency $\bar{\Omega}$ have been evaluated (Hughes, 1987). Nonetheless, a complementary characterization of the novel integrators was performed through digital control theory and the bilinear transformation used for creating digital filters,

$$w = \frac{1}{\Delta t} \frac{z-1}{z+1} \tag{2.3}$$

where the factor 2 at the numerator, that is usually exploited to properly obtain the poles in the trapezium rule has been omitted to avoid further assumptions. As a result, the poles of the LSRT2 method and those of the G-α method with $\rho_\infty=0$ including spurious roots can be represented in the Argand-Gauss plane as shown in Figure 3(a) and 3(b), respectively. One can observe the damping effect for the LSRT2 method that is lower with respect to that of the G-α method; as well as the presence of a spurious root for the G-α method.

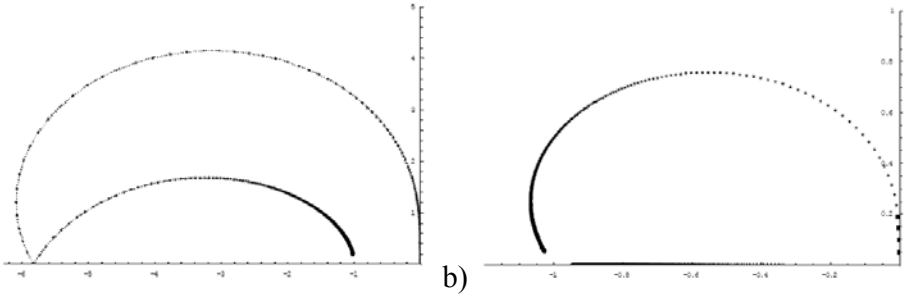

a) b)

Figure 3 Representation of the poles in the Argand-Gauss plane for a second-order mechanical system with ξ=0 for: a) the LSRT2 method; b) the G-α method with $\rho_\infty=0$.

The LSRT algorithms are endowed with several favourable characteristics: (i) they can be implemented in a real time environment being linearly implicit, noniterative and with fixed time steps; (ii) they can deal with stiff systems through the L-stability property; (iii) they do not exhibit overshoot in the velocity for large time steps; (iv) they predict explicitly the state, thus they can control better the dynamics of the transfer system.

2.2 Application of LSRT2 algorithms to non-linear RTDS tests

In this section, we apply the LSRT2 methods to non-linear RTDS tests. In this application, the transfer system

consists of an electrically driven ball-screw actuator with an in-line mounted servo-motor controlled by a servo-drive which applies a displacement to the PS in the vertical direction. The complete system represents a 3-DoF spring pendulum non-linear system and is shown and schematized with its NS and PS in Figure 4.

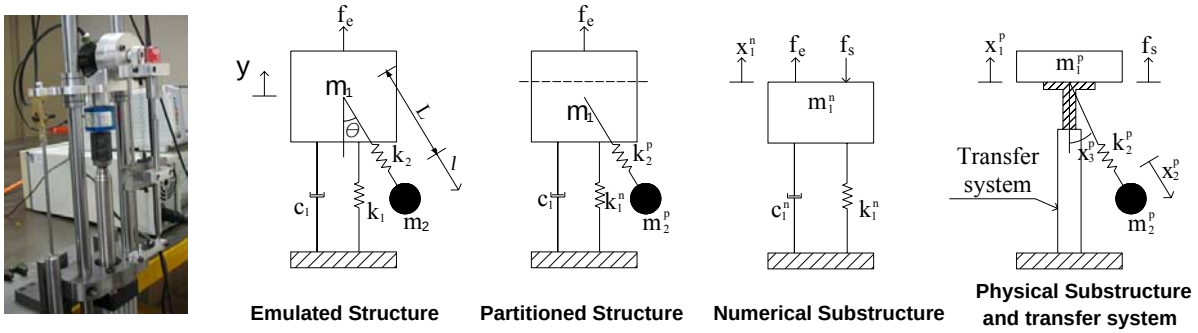

Figure 4 View and schematic representation of a 3-DoF system with dynamic substructuring

The system consists of a spring pendulum with its pivot point connected to the mass m_1^p, belonging to a mass-spring-damper. The pendulum mass, m_2^p, is assumed to act at a single point and is connected to the pivot point by a spring, k_2^p. In all the experiments presented here the transfer system dynamics are controlled by means of a PID controller and a polynomial delay compensation technique (Wallace *et al.* 2005). The parameter values of the system are collected in Table 2.1. The NS is a linear mass-spring-damper in System 1; whilst it is a non-linear system governed by a Bouc-Wen model (Bonelli and Bursi 2004) in System 2.

Table 2.1 Characteristics of non-linear substructured systems

	m_1^n [kg]	c_1^n [kg/s]	B-W model	k_1^n [N/m]	m_1^p [kg]	c_1^p [kg/s]	m_2^p [kg]	c_2^p [kg/s]	k_2^p [N/s]	l_{sp} [m]
System 1	16	40		1000	1	50	0.34	1.4	400	0.167
System 2	10	10	β=55, α=45 K_0=1000	1000	1	50	0.34	1.4	400	0.167

The behaviour of System 1 using the LSRT2 method and assuming Δt=0.002s is plotted in Figure 5. The capability of the LSRT2 method to deal with a non-linear spring-pendulum system endowed with large oscillations is evident.

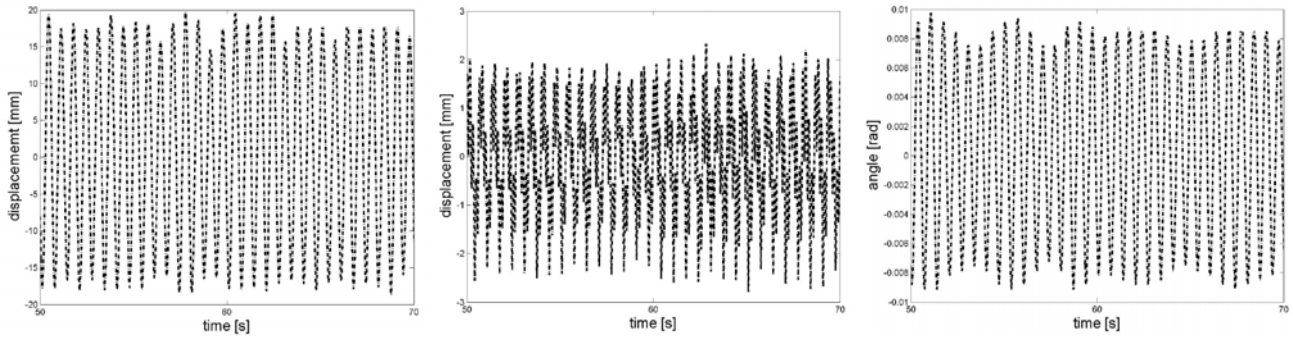

Figure 5: Experimental results for System 1 excited by a force with f=1.5Hz and A=15N integrated by the LSRT2 method: displacement of mass 1; displacement of mass 2; rotation of pendulum.

The response of the 3 DoFs system with a non-linear NS using the LSRT2 method and assuming Δt=0.002s is plotted in Figure 6 for different external forces. In detail, the force is a sinusoid with frequency 1.2Hz and amplitude 20N in Figure 6a; whilst it is a sinusoid with frequency 2.2Hz and amplitude 30N in Figure 6b. In the first case, the frequency of the external force is in resonance with the non-linear NS, thus inducing a strong hysteretic behaviour. In the second case, the frequency of the external force is closer to the natural frequencies of the spring-pendulum system; in fact, the vertical displacement of the second mass and the rotation of the pendulum show larger values compared to the previous simulation. In sum, both tests confirm the capability of

the LSRT2 method to deal with non-linearity both in the NS and in the PS. Moreover, the application of the proposed algorithms and other structural integrators, like the Explicit Newmark-β method and the linearly implicit Chang method (Bonnet *et al.* 2007), to stiff systems simulated numerically can entail instability owing to the lack of sufficient numerical damping.

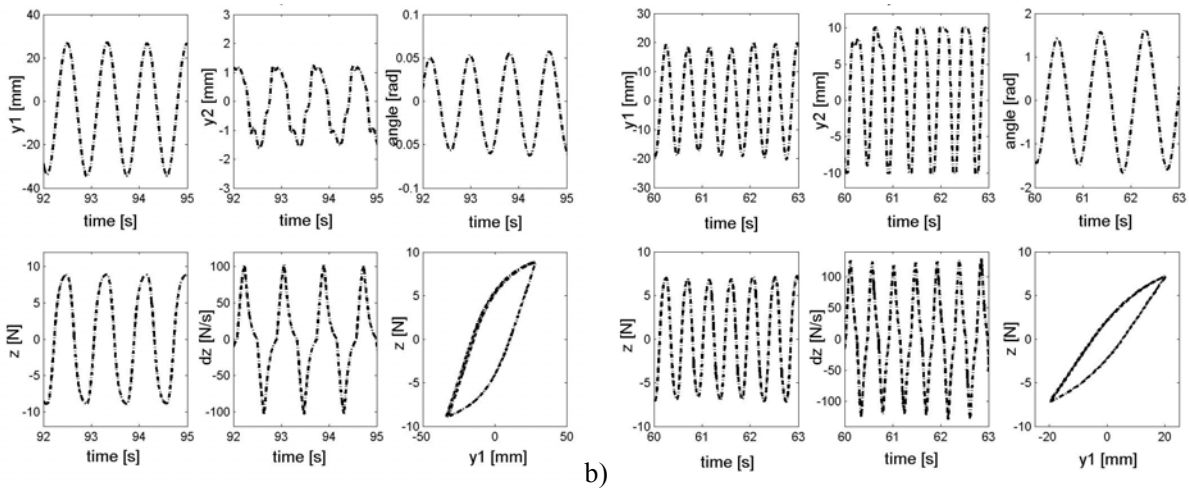

Figure 6: Response of System 2 integrated by the LSRT2 method and excited with a sinusoid of a) f=1.2Hz and A=20N; b) f=2.2Hz and A=30N.

3. AN INTERFIELD PARALLEL INTEGRATOR BASED ON THE GENERALIZED-α METHOD

3.1 Governing equations for the partitioned problem

In this section, we consider a dual Schur domain decomposition following Gravouil and Combescure (2001). By partitioning a structural domain into *sd* subdomains, the following semi-discrete dynamic system of equations of motion is obtained:

$$\mathbf{M}^i\ddot{\mathbf{u}}^i(t)+\mathbf{C}^i\dot{\mathbf{u}}^i(t)+\mathbf{K}^i\mathbf{u}^i(t)=\mathbf{F}_e^i(t)+\mathbf{L}^{i^T}\boldsymbol{\Lambda}(t) \qquad \forall i\in\{1,\cdots,sd\} \tag{3.1}$$

$$\sum_i^{sd}\mathbf{L}^i\dot{\mathbf{u}}^i(t)=\mathbf{0} \tag{3.2}$$

where $\mathbf{M}^i$, $\mathbf{C}^i$ and $\mathbf{K}^i$ are the subdomain mass, damping and stiffness matrices, respectively; $\mathbf{F}^i_e(t)$ is the vector of applied loads on the *i*-th subdomain; $\mathbf{u}^i(t)$ is the *i*-th subdomain displacement vector and superimposed dots indicate time differentiation; $\mathbf{L}^i$ are the constraint matrices that express a linear relationship on the connected boundaries and $\boldsymbol{\Lambda}(t)$ is the vector of Lagrange multipliers. (3.1) and (3.2) result in a system of differential-algebraic equations (DAEs). In the following we consider for simplicity *sd*=2 as shown in Figure 2.

3.2 Generalized-α methods with equilibrium conditions enforced at the end of each time step

The PM method with the Trapezium Rule and the Central Difference is numerically nondissipative with a common time step and entails numerical dissipation only at interfaces with different time steps in different subdomains (Bonelli et al., 2008); moreover, it is not user-controllable. Even though the Newmark-β methods with γ-damping (Hughes, 1987) can be applied to the PM method, the algorithm becomes over-dissipative in the low frequency range and provides poorly accurate results (He, 2008). To obtain controllable numerical dissipation, we properly introduce the G-α methods into the PM method. The progenitor implicit (Chung and Hulbert, 1993) and explicit (Hulbert and Chung, 1996) G-α methods, that enforce equilibrium conditions using a balanced equation between two consecutive time steps, have been found incompatible with the dual Schur domain decomposition (3.1)-(3.2). Instabilities arouse owing to the weak continuity enforcement via Lagrange multipliers. As a result, we employ the G-α method in the implicit subdomain enforcing the equilibrium at the

end of each coarse time step along the lines of Arnold and Bruls (2007). Further, we propose an explicit G-α method in the explicit subdomain that also enforces equilibrium at the end of each time step. In view of the implementation, we consider herein a predictor-corrector (PC) form of the implicit G-α method:
Predictors:

$$\tilde{\mathbf{u}}_n = \mathbf{u}_n + \Delta t\dot{\mathbf{u}}_n + \Delta t^2(\frac{1}{2} - \frac{\beta}{1-\alpha_m})\mathbf{a}_n + \Delta t^2\frac{\beta\alpha_f}{1-\alpha_m}\ddot{\mathbf{u}}_n,\ \tilde{\dot{\mathbf{u}}}_n = \dot{\mathbf{u}}_n + \Delta t(1-\frac{\gamma}{1-\alpha_m})\mathbf{a}_n + \Delta t\frac{\gamma\alpha_f}{1-\alpha_m}\ddot{\mathbf{u}}_n \tag{3.3}$$

Equilibrium equation:

$$\mathbf{M}\ddot{\mathbf{u}}_{n+1} + \mathbf{C}\dot{\mathbf{u}}_{n+1} + \mathbf{K}\mathbf{u}_{n+1} = \mathbf{F}_{e,n+1} \tag{3.4}$$

Correctors:

$$\mathbf{u}_{n+1} = \tilde{\mathbf{u}}_n + \Delta t^2\frac{\beta(1-\alpha_f)}{1-\alpha_m}\ddot{\mathbf{u}}_{n+1},\ \dot{\mathbf{u}}_{n+1} = \tilde{\dot{\mathbf{u}}}_n + \Delta t\frac{\gamma(1-\alpha_f)}{1-\alpha_m}\ddot{\mathbf{u}}_{n+1} \tag{3.5}$$

Recursive equation:

$$(1-\alpha_m)\mathbf{a}_{n+1} + \alpha_m\mathbf{a}_n = (1-\alpha_f)\ddot{\mathbf{u}}_{n+1} + \alpha_f\ddot{\mathbf{u}}_n,\ \mathbf{a}_0 = \ddot{\mathbf{u}}_0 \tag{3.6}$$

Moreover, to obtain the explicit G-α method we propose the following equilibrium equation:

$$\mathbf{M}\ddot{\mathbf{u}}_{n+1} + \mathbf{C}\dot{\mathbf{u}}_{n+1} + \mathbf{K}\tilde{\mathbf{u}}_n = \mathbf{F}_{e,n+1} \tag{3.7}$$

Equations (3.3), (3.5)-(3.7) provide an explicit implementation of the G-α method. For the solution procedure, both the implicit and the explicit G-α methods can be implemented in the following $\ddot{\mathbf{u}}$-form:

$$\tilde{\mathbf{M}}\ddot{\mathbf{u}}_{n+1} = \mathbf{F}_{e,n+1} - \mathbf{C}\tilde{\dot{\mathbf{u}}}_n - \mathbf{K}\tilde{\mathbf{u}}_n \tag{3.8}$$

where for the implicit and explicit methods,

$$\tilde{\mathbf{M}} = \tilde{\mathbf{M}}^I = \mathbf{M} + \Delta t\frac{\gamma(1-\alpha_f)}{1-\alpha_m}\mathbf{C} + \Delta t^2\frac{\beta(1-\alpha_f)}{1-\alpha_m}\mathbf{K},\ \tilde{\mathbf{M}} = \tilde{\mathbf{M}}^E = \mathbf{M} + \Delta t\frac{\gamma(1-\alpha_f)}{1-\alpha_m}\mathbf{C}, \tag{3.9}$$

respectively. After (3.8) is solved in each time step, the solution of $\mathbf{u}_{n+1}$, $\dot{\mathbf{u}}_{n+1}$ and $\mathbf{a}_{n+1}$ are updated through (3.5) and (3.6). Proper choices about the integration parameters of the explicit method are provided in He (2008).

3.3 Novel interfield parallel algorithm using the Generalized-α methods

The main challenge in multi-time-step integration is to properly account for the coupling between state variables integrated at different rates in different subdomains. In this respect, we follow here a specific PC approach proposed by Gravouil and Combescure (2001) and known as the free-link approach. Thus in each subdomain, the integration using the G-α methods is decoupled into a free problem and a link problem:

$$\tilde{\mathbf{M}}^i\ddot{\mathbf{u}}^i_{n+1,f} = \mathbf{F}^i_{e,n+1} - \mathbf{C}^i\tilde{\dot{\mathbf{u}}}^i_n - \mathbf{K}^i\tilde{\mathbf{u}}^i_n,\ \mathbf{u}^i_{n+1,f} = \tilde{\mathbf{u}}^i_n + \alpha^i_1\ddot{\mathbf{u}}^i_{n+1,f},\ \dot{\mathbf{u}}^i_{n+1,f} = \tilde{\dot{\mathbf{u}}}^i_n + \alpha^i_2\ddot{\mathbf{u}}^i_{n+1,f} \tag{3.10}$$

$$\tilde{\mathbf{M}}^i\ddot{\mathbf{u}}^i_{n+1,l} = \mathbf{L}^{i^T}\mathbf{\Lambda}_{n+1},\ \mathbf{u}^i_{n+1,l} = \alpha^i_1\ddot{\mathbf{u}}^i_{n+1,l},\ \dot{\mathbf{u}}^i_{n+1,l} = \alpha^i_2\ddot{\mathbf{u}}^i_{n+1,l} \tag{3.11}$$

with $\alpha^i_1 = \Delta t^2_i\frac{\beta_i(1-\alpha^i_f)}{1-\alpha^i_m}$ and $\alpha^i_2 = \Delta t_i\frac{\gamma_i(1-\alpha^i_f)}{1-\alpha^i_m}$. Here, subscripts f and l denote the free and link problems, respectively. The original kinematic quantities are obtained by summing free and link quantities, i.e., $(\ ) = (\ )_f + (\ )_l$. Thus, a free problem is solved in each subdomain that does not require information of constraints between subdomains; then the Lagrange multipliers are solved to define the link problem. Due to the different time scales between A and B, the projections from the coarse time step to the fine time step are defined in terms of a linear interpolation (Gravouil and Combescure, 2001):

$$\dot{\mathbf{u}}^A_{n+j/ss,f} = (1-\frac{j}{ss})\dot{\mathbf{u}}^A_{n,f} + \frac{j}{ss}\dot{\mathbf{u}}^A_{n+1,f},\ \dot{\mathbf{u}}^A_{n+j/ss,l} = (1-\frac{j}{ss})\dot{\mathbf{u}}^A_{n,l} + \frac{j}{ss}\dot{\mathbf{u}}^A_{n+1,l},\ \mathbf{\Lambda}_{n+j/ss} = (1-\frac{j}{ss})\mathbf{\Lambda}_n + \frac{j}{ss}\mathbf{\Lambda}_{n+1},\quad \forall j \in \{1,\cdots,ss\} \tag{3.12}$$

As a result, the continuity relationship (3.2) can be rewritten as

$$\mathbf{L}^A\dot{\mathbf{u}}^A_{n+j/ss,l}+\mathbf{L}^B\dot{\mathbf{u}}^B_{n+j/ss,l}=-(\mathbf{L}^A\dot{\mathbf{u}}^A_{n+j/ss,f}+\mathbf{L}^B\dot{\mathbf{u}}^B_{n+j/ss,f}) \tag{3.13}$$

By considering (3.11)-(3.12), one obtains from (3.13) a condensed global problem at the interfaces:

$$\mathbf{H}\boldsymbol{\Lambda}_{n+j/ss}=-(\mathbf{L}^A\dot{\mathbf{u}}^A_{n+j/ss,f}+\mathbf{L}^B\dot{\mathbf{u}}^B_{n+j/ss,f}) \tag{3.14}$$

with $\mathbf{H}=\alpha_2^A\mathbf{L}^A\tilde{\mathbf{M}}^{A^{-1}}\mathbf{L}^{A^T}+\alpha_2^B\mathbf{L}^B\tilde{\mathbf{M}}^{B^{-1}}\mathbf{L}^{B^T}$. In a greater detail, the method for advancing from t_{n-1} to t_{n+1} in the subdomain A and from t_n to t_{n+1} in the subdomain B can be summarized by the following pseudo-code:

1. solve the free problem (3.10) in subdomain A by using $2\Delta t_A$, thus advancing from t_{n-1} to t_{n+1};
2. start the loop on *ss* substeps in subdomain B;
3. solve (3.10) in subdomain B by using Δt_B, thus advancing from $t_{n+(j-1)/ss}$ to $t_{n+j/ss}$ with $j = \{1,\ldots,ss\}$;
4. interpolate the free velocity $\dot{\mathbf{u}}^A_{n+j/ss,f}$ in subdomain A according to (3.12);
5. compute the Lagrange multipliers $\boldsymbol{\Lambda}_{n+j/ss}$ by solving the condensed global problem (3.14);
6. solve the link problem (3.11) in subdomain B at $t_{n+j/ss}$;
7. compute kinematic quantities in subdomain B at $t_{n+j/ss}$ by summing free and link quantities;
8. if $j = ss$, then end the loop in subdomain B;
9. solve the link problem (3.11) in subdomain A by using $2\Delta t_A$, from t_{n-1} to t_{n+1};
10. compute kinematic quantities in subdomain A at t_{n+1} by summing free and link quantities.

The ongoing interfield process in the subdomains A and B is inherently parallel as depicted by dash-dot lines in Figure 2. Hereafter, we refer to the proposed method as the PM-α method.

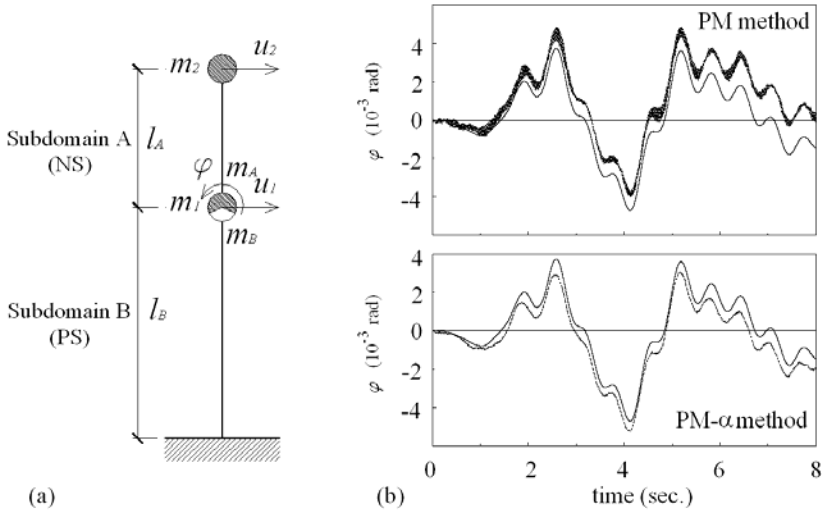

Figure 7 Partitioned three-DoF system: a) model problem; b) rotational response provided by the PM (upper) and PM-α method (lower) methods with (dotted lines) and without (solid lines) error effects

3.4 Representative numerical experiments

In order to highlight the high-frequency numerical dissipation of the PM-α method applied to PsD testing, we consider a partitioned three-DoF system shown in Figure 7a. The displacement vector of subdomain A is chosen to be $\mathbf{U}_A=\{u_1, \varphi, u_2\}^T$, whilst that of subdomain B is chosen as $\mathbf{U}_B=\{u_1, \varphi\}^T$. The emulated system is endowed with the following natural frequencies: f_1=0.25 Hz, f_2=1.6 Hz and f_3=70 Hz. The emulated structure is subjected to the El Centro ground motion with a 0.35g p.g.a.. Subdomain A is regarded as the NS, whilst subdomain B is taken as the PS. The structural response is integrated by both the PM method and the PM-α method. Moreover, two kinds of experimental errors are considered in the PS: the measurement errors of the load cells simulated by means of white noises and undershooting errors resulting from the displacement control of the actuators. The same time step Δt_B=0.02ms and ss=100 are employed for both methods.

Figure 7b shows the rotational response of the emulated structure with and without experimental error effects. It is evident that the high-frequency components of the response are falsely excited by the experimental errors. The PM method without the user-controllable numerical dissipation, traces the unwanted high-frequency components of the response, whilst they are effectively annihilated by the PM-α method.

4. CONCLUSIONS

In this paper, we have presented novel linearly implicit noniterative real-time compatible integration algorithms based on the Rosenbrock methods for non-linear coupled systems. In detail, we proved the efficiency of these L-stable algorithms in non-linear real time tests with dynamic substructuring. Despite the need to compute a Jacobian operator at the beginning of each time step, the proposed algorithms are more competitive than traditional structural integrators. Furthermore, we extended the effectiveness of the interfield parallel PM method used in pseudo-dynamic testing by means of the G-α methods. Simulations showed that unwanted high-frequency components of the response were effectively annihilated by the novel PM-α method.

REFERENCES

Arnold M. and Bruls O. (2007). Convergence of the Generalized-α scheme for constrained mechanical systems. *Multibody Syst. Dyn.*, **18**: 185–202.

Bonelli A. and Bursi O.S. (2004). Generalized-alpha Methods for Seismic Structural Testing. *Earthquake Engineering and Structural Dynamics*, **33**: 1067-1102.

Bonelli A., Bursi O.S., He L., Pegon P. and Magonette G. (2008). Convergence analysis of a parallel interfield method for heterogeneous simulations with dynamic substructuring. *International Journal for Numerical Methods in Engineering*, **75:7**, 800-825.

Bonnet P.A., Williams M.S., Blakeborough A. (2008). Evaluation of numerical time-integration schemes for real-time hybrid testing. *Earthquake Engineering and Structural Dynamics*, 10.1002/eqe.821.

Burgermeister, B., Arnold M., Esterl, B. (2006). DAE time integration for real-time applications in multi-body dynamics. *Z. Angew. Math. Mech*. **86**, 759–771.

Bursi O.S., Gonzalez-Buelga A., Vulcan L., Neild S.A. and Wagg D.J. (2008). Novel coupling Rosenbrock-based algorithms for real-time dynamic substructure testing. *Earthquake Engineering and Structural Dynamics,* **37**: 339-360.

Chung J. and Hulbert G. (1993). A time integration algorithm for structural dynamics with improved numerical dissipation: the Generalized-α method. *Journal of Appl. Mech.*, **60**: 371-375.

dSPACE (2001). dSPACE. *Real-time Interface, Implementation Guide, Release 3.2*. Paderborn, Germany.

Gravouil A. and Combescure A. (2001). Multi-time-step explicit-implicit method for non-linear structural dynamics. *International Journal for Numerical Methods in Engineering*, **50:1**, 199–225.

He L. (2008). *Development of Partitioned Time Integration Schemes for Parallel Simulation of Heterogeneous Systems*. PhD thesis, University of Trento.

Hughes T.J.R. (1987). *The Finite Element Method, Linear Static and Dynamic Finite Element Analysis*. Prentice-Hall, Englewood Cliffs, NJ.

Hulbert G.M. and Chung J. (1996). Explicit time integration algorithms for structural dynamics with optimal numerical dissipation. *Comp. Meth. Appl. Mech. Eng.*, **137**: 175–188.

Pegon P. and Magonette G. (2002). Continuous PSD testing with non-linear substructuring: presentation of a stable parallel inter-field procedure. *Technical Report I.02.167*, E.C., Joint Research Centre, ELSA, Ispra, Italy.

Rosenbrock H.H. (1963). Some general implicit processes for the numerical solution of differential equations. *Computer Journal*, **5:4**, 329–330.

Wallace M.I., Wagg D.J. and Neild S.A. (2005). An adaptive polynomial based forward prediction algorithm for multi-actuator real-time dynamic substructuring. *Proc. of the Royal Soc. A*, **461:2064**, 3807–3826.

Williams M.S. and Blakeborough A. (2001). Laboratory testing of structures under dynamic loads: an introductory review. *Philosophical Transactions of the Royal Society A*, **359:1786**, 1651–1669.